

Article

Research and Development of Online Monitoring Protection Sensors for Paper Books Based on TiO₂ NT/MoS₂

Jia Wang ^{1,*}, Lifang Ke ², Jieling Wu ², Feng Liang ² and Yanxiong Xiang ²¹ Library, Lingnan Normal University, Zhanjiang 524048, China² Key Laboratory of Advanced Coating and Surface Engineering, Lingnan Normal University, Zhanjiang 524048, China; lifangkeshangan@163.com (L.K.); wujieling666888@163.com (J.W.); lingf@lingnan.edu.cn (F.L.); xiangyx@lingnan.edu.cn (Y.X.)

* Correspondence: wangjia@lingnan.edu.cn

Abstract: NO₂ is a prevalent environmental pollutant, and its reaction with water produces nitric acid, which is one of the main factors contributing to the degradation of books and paper. Therefore, it is crucial to develop a real-time monitoring system for NO₂ gas content in the air and establish timely response measures to delay book aging and provide effective protection. In this study, TiO₂ nanotubes (NTs) were fabricated using the anodic oxidation method, followed by the preparation of TiO₂ NT/MoS₂ composites through hydrothermal synthesis. It was observed that flaky MoS₂ is attached to the surface of TiO₂ nanotubes, forming aggregated structures resembling flower balls. The TiO₂ NT/MoS₂ nanocomposites were found to exhibit a rapid response with a 5 s response time and an 80 s recovery time towards 367 ppm NO₂ at 260 °C. The gas response to 100 ppm NO₂ vapor was 3.3, which is higher than all the other gases under the same concentration. Our experimental results demonstrate that compared to pure TiO₂ NTs, TiO₂ NT/MoS₂ composites exhibit a larger specific surface area along with higher sensitivity and faster response times towards various concentrations of NO₂ gas.

Keywords: TiO₂ NTs; MoS₂; NO₂ gas sensor; gas-sensitive properties

Citation: Wang, J.; Ke, L.; Wu, J.; Liang, F.; Xiang, Y. Research and Development of Online Monitoring Protection Sensors for Paper Books Based on TiO₂ NT/MoS₂. *Coatings* **2024**, *14*, 552. <https://doi.org/10.3390/coatings14050552>

Academic Editor: Csaba Balázs

Received: 21 March 2024

Revised: 16 April 2024

Accepted: 16 April 2024

Published: 30 April 2024



Copyright: © 2024 by the authors. Licensee MDPI, Basel, Switzerland. This article is an open access article distributed under the terms and conditions of the Creative Commons Attribution (CC BY) license (<https://creativecommons.org/licenses/by/4.0/>).

1. Introduction

With the advancement of human civilization, the paramount importance of paper books in libraries and museums has been increasingly recognized. Serving as conduits for information dissemination, paper books not only retain their value and significance over time but also witness a gradual augmentation. However, as time elapses, books are susceptible to acidification and mold growth due to dust erosion and air pollution gases, ultimately leading to a loss in the mechanical strength of the paper medium and compromising the preservation of valuable information [1]. Consequently, it becomes imperative to implement rapid and effective real-time monitoring and control measures for various gases within libraries in order to mitigate book aging. The dissolution of NO₂ gas into water generates nitric acid, which possesses both acidity properties and strong oxidizing capabilities. This acidic nature corrodes the cellulose present in paper, while its potent oxidation potential accelerates cellulose degradation, thereby expediting book aging [2]. When the humidity in a library increases, the hydrophilic nature of paper fibers and the high moisture absorption of capillaries on the paper surface lead to an increase in water content. This makes it easier for harmful gases dissolved in water to be adsorbed by the paper, increasing the conversion of these gases into acids and causing yellowing and brittleness. Therefore, developing a NO₂ gas-sensitive sensor that is swift yet accurate holds immense practical significance.

The detection of gases using metal oxide semiconductor gas-sensitive sensors involves measuring changes in physical properties, such as conductivity, when the target gas interacts with the sensor components. These sensors possess characteristics including high

sensitivity, short response and recovery times, a simple fabrication process, low cost, and a long lifespan [3,4]. TiO₂ nanotubes (NTs), a popular semiconductor material, offer advantages such as large potential difference, excellent photochemical performance without corrosion issues, and high photocatalytic activity for repeated use. They can be utilized as gas sensors to detect various gases [5]. However, TiO₂ sensors face challenges of operating at high temperatures and exhibiting low sensitivity in the absence of catalysts [5]. MoS₂ possesses benefits like high electron mobility, a large specific surface area, good thermal stability, and high sensitivity [6], enabling it to detect very low concentrations of gases. Therefore, combining TiO₂ NTs with MoS₂ can enhance gas sensitivity while significantly reducing the optimal operating temperature required [7]. It is noteworthy that the modification of TiO₂ with 2D nanomaterials becomes an effective route that can be used to improve the inherent properties of TiO₂ toward gas detection [8,9]. The improved photodegradation activity and gas-sensing performance of MoS₂/TiO₂-NA heterojunction nanohybrids were reported upon UV-visible light irradiation [10]. The sensing mechanism of the Pd-TiO₂/MoS₂ sensor was attributed to the synergistic effect of the ternary nanostructures, combining the modulation of potential barriers with electron transfer [11]. A low-dimensionality MoS₂/TiO₂ composite was synthesized using the hydrothermal method, and the response and recovery times were as high as 52 s and 155 s [12]. The novel features of MoS₂/TiO₂ heterojunction not only take the advantages of TiO₂ nanotubes (e.g., fast electron transportation through vertical tube walls and high effective surface area), facilitating a higher number of adsorption sites, but they can also potentially present localized highly reactive areas via MoS₂ modification and thus achieve unexpected characteristics for sensing applications [13]. However, to the best of our knowledge, only a few studies have been published on the MoS₂/TiO₂ heterojunction on gas/vapor sensing performance.

Based on this premise, the present study employs the anodic oxidation method to prepare TiO₂ NTs, followed by hydrothermal synthesis to obtain a composite of TiO₂ NT/MoS₂ which is used as the gas-sensitive material for gas-sensitive sensors [14,15]. The sensitivity of this composite towards different concentrations of gases is evaluated using NO₂ as a common acid gas. By investigating its response towards acid gases, we aim to identify a highly sensitive gas sensing material that can efficiently and accurately monitor acid gases in ambient air, thereby mitigating book aging.

2. Preparation and Characterization of Gas-Sensitive Materials

2.1. Preparation of TiO₂ NTs

TiO₂ NTs were prepared using the anodic oxidation method [16]. First, high-purity Ti sheets (with a Ti mass fraction of 99.99%) were pretreated via chemical polishing and physical ultrasonic cleaning, and then cut into 1 × 5 cm². The Ti sheets were polished with 400, 800, 1200, 1500, and 2000 mesh sandpaper to remove the oxidation film on the surface of the Ti sheets until there were no scratches on the surface. The polished Ti sheets were cleaned with acetone, anhydrous ethanol, and deionized water for 10 min, and then 1 L of ethylene glycol, 2 g of ammonium fluoride, and 100 mL of deionized water were weighed to prepare the organic electrolyte. The pretreated Ti sheets were used as the anode and graphite as the cathode, and the distance between the two poles was adjusted to 3 cm. Then, the constant high voltage of 40 V was applied for 30 min, the voltage was then adjusted to 10 V for 10 min, and finally the voltage was adjusted back to 40 V. The reaction was carried out at room temperature for 3 h. The Ti sheets were cleaned with deionized water and anhydrous ethanol and then dried, and the TiO₂ NT array was obtained. The surface activity of ethanol molecules at the interface of water and particulate substances enables ethanol to effectively disperse the particulate substances and maintain their dispersed state. After the samples were dried, the samples were cleaned with deionized water, and the samples were heat-treated at 500 °C for 5 h to complete the transformation of TiO₂ from amorphous to anatase crystal type [17].

2.2. Preparation of TiO₂ NT/MoS₂ Nanocomposites

The TiO₂ NT/MoS₂ composites were prepared via a hydrothermal method [18]. Initially, 0.02918 g, 0.1458 g, and 0.0728 g of thiourea were weighed along with 0.1960 g, 0.0988 g, and 0.0494 g of sodium molybdate, respectively. Subsequently, 80 mL of deionized water was added to the beaker, followed by the sequential addition of sodium molybdate and thiourea. Meanwhile, stirring was carried out with a magnetic stirrer for uniform mixing for a duration of 30 min. Afterward, monohydrated citric acid (10 mL) was introduced into the beaker and stirred continuously for another half an hour before subjecting the solution to ultrasonic treatment for ten minutes. The resulting solution was transferred into a liner (100 mL) and was then placed inside a reaction kettle and subjected to hydrothermal reaction at 150 °C for a period of twenty-four hours in an oven-dry environment. Following this step, the liner containing the composite product at its bottom was removed from the reaction kettle and washed repeatedly with deionized water and anhydrous ethanol until pH neutrality was achieved in the aqueous solution (pH = 7). Finally, drying took place in an oven set at 80 °C over twelve hours.

2.3. Preparation of the Online Monitoring Sensor

Initially, 20 mg of composite powder was accurately weighed and evenly spread onto a fingertip electrode. The electrode was then placed into a weighing bottle. Subsequently, 1 mL of anhydrous ethanol was carefully pipetted onto the electrode sheet to dissolve the powder into a solution, followed by ultrasonic cleaning for the 10 min. Next, the weighing bottle containing the electrode was positioned in a water bath and heated to 90 °C for 30 min to evaporate the solvent and ensure the uniform deposition of powder on the electrode surface. The online monitoring sensor system is shown in Figure 1. The experimental setup consisted of various components, including a computer, vacuum cavity, digital source meter, air pump, probe, gas flowmeter, temperature controller, and gas bag for testing purposes. Prior to conducting the experiments, the prepared gas-sensitive components were placed on the detection platform within the vacuum cavity. The temperature controller was adjusted accordingly to achieve the desired experimental conditions within the cavity. Once reaching the target temperature, as indicated by a thermometer reading, NO₂ gas was introduced into the reaction chamber by opening the ventilation valve, allowing adsorption reactions between NO₂ molecules and the surface of gas-sensitive components to occur. During the experimentation process, variations in inflow concentrations or cavity temperatures caused changes in resistance values exhibited by these gas-sensitive components which were subsequently analyzed using response–recovery time curves.

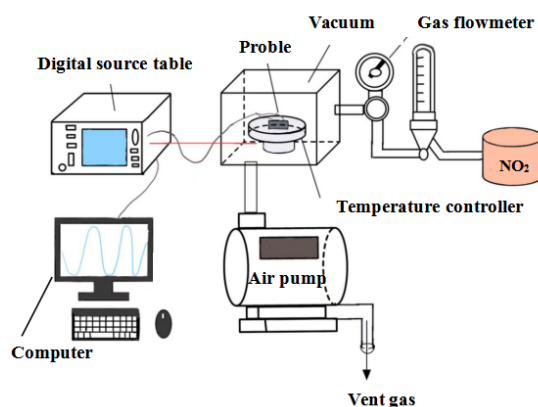


Figure 1. Schematic diagram of the online monitoring sensor.

3. Analysis and Discussion

3.1. Phase Analysis of TiO₂ NTs and TiO₂ NT/MoS₂ Composites

XRD was used to analyze the prepared TiO₂ NTs, MoS₂, and TiO₂ NT/MoS₂ nanocomposites, and the results are shown in Figure 2. Figure 2a indicates that the diffraction

pattern of TiO₂ NTs corresponded to the standard JCPDS card (No. 84-1285) with an anatase structure. The (101), (004), (200), (105), (204), and (116) characteristic peaks of anatase appeared at $2\theta = 25.21^\circ$, 37.85° , 47.93° , 54.02° , 62.82° , and 68.88° , respectively [19]. Figure 2b indicates that the diffraction pattern of MoS₂ corresponded to the standard JCPDS card (No. 89-5112) with a hexagonal phase. The characteristic peaks of MoS₂ (104), (103), (202), and (119) crystal faces appeared at $2\theta = 38.15^\circ$, 40.07° , 70.43° , and 76.05° , respectively. As shown in Figure 3c, the characteristic peaks of TiO₂ NT (101) crystal faces appeared at $2\theta = 25.17^\circ$, and the characteristic peaks of MoS₂ (104) and (103) appeared at $2\theta = 38.15^\circ$ and 40.07° , indicating that there are two phases of TiO₂ NTs and MoS₂. As shown in Figure 2b, with a decrease in sodium molybdate concentration, the characteristic peaks of MoS₂ (104) and (103) gradually weakened. With the assistance of MoS₂, oxygen molecules can be more easily adsorbed on the surface of TiO₂ nanotubes.

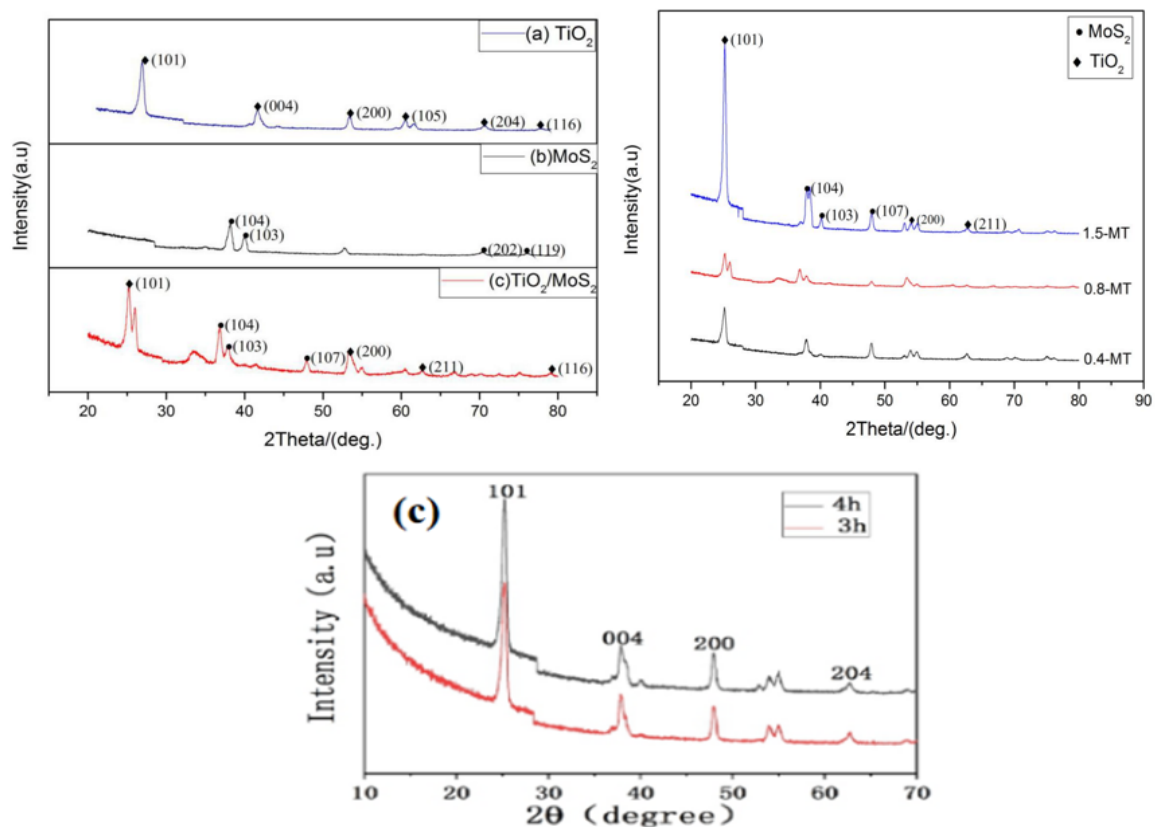


Figure 2. XRD patterns of TiO₂ NT/MoS₂ (a), TiO₂ NT/MoS₂ with different molybdate concentrations (b), and TiO₂ NTs with oxidation times of 3 and 4 h (c).

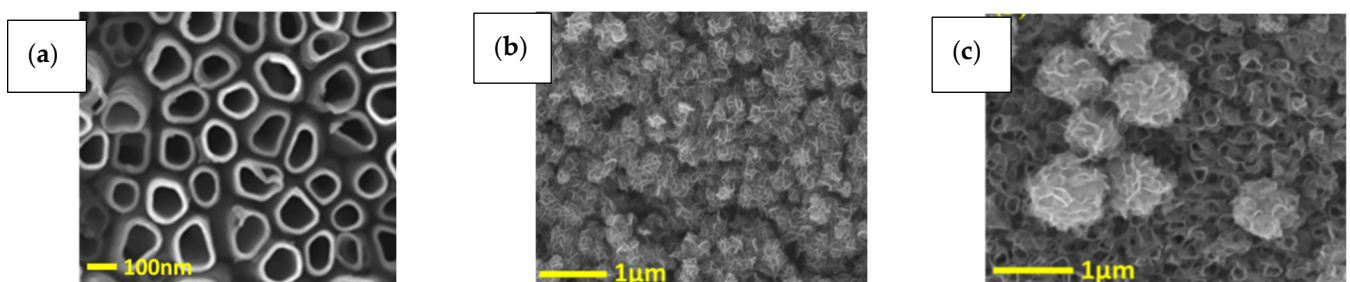


Figure 3. (a) SEM image of pure TiO₂ NTs; (b) SEM image of MoS₂ loaded on un-anodized Ti; (c) SEM image of TiO₂ NT/MoS₂ nanocomposites.

The XRD pattern analysis of TiO₂ NTs at different oxidation times is presented in Figure 2c. As depicted, the diffraction peaks observed at 2θ values of 25.2°, 37.8°, 47.9°, 53.0°, 54.9°, and 62.7° corresponded to the crystallographic planes (101), (004), (200), (105), (211), and (204) of the anatase phase, respectively. Based on the calibration results of XRD patterns, the crystallographic planes (101), (102), and (103) of titanium were identified by their respective peak positions at 2θ values of 40.2°, 53.0°, and 70.7°, confirming that TiO₂ in the prepared sample existed predominantly in anatase form with excellent crystallinity properties. It is noteworthy that the characteristic diffraction peak corresponding to a four-hour oxidation time exhibited enhanced sharpness indicative of superior crystallization quality for the TiO₂ NT nanocomposites. The TiO₂ nanotubes oxidized for 4 h with superior crystallization quality for the TiO₂ indicates a significant enhancement in the effective oxide surface area that may facilitate the adsorption of target molecules, which is beneficial for the gas sensing properties of the TiO₂ NTs.

3.2. Morphology and Element Analysis

The morphology of the sample was observed using scanning electron microscopy (SEM), and the chemical composition was analyzed using energy-dispersive X-ray spectroscopy (EDS, Hitachi, S-4800, Tokyo, Japan). The results are presented in Figure 3, where Figure 3a depicts the SEM spectrum of pure TiO₂ nanotubes with an average diameter of approximately 140 nm. Figure 3b shows the SEM spectrum of MoS₂ loaded onto a non-anodized Ti sheet, while Figure 3c displays the SEM spectrum of the TiO₂ nanotube/MoS₂ nanocomposites. It can be observed that flaky MoS₂ was attached to the surface of TiO₂ nanotubes, forming aggregated structures resembling flower balls. This aggregation phenomenon is attributed to the addition of hydrated citric acid during the hydrothermal synthesis process, which acts as an adsorbent in promoting particle agglomeration. The hydrated citric acid has the effect of promoting chemical reactions and particle agglomeration, leading to the rapid formation of TiO₂/MoS₂ nanocomposites. With the assistance of MoS₂, oxygen molecules can be more easily adsorbed on the surface of TiO₂ nanotubes. This process increases both the quantity of adsorbed oxygen and the molecule–ion conversion rate, resulting in a greater and faster degree of electron depletion from the TiO₂, which would lead to a decrease in the response time for TiO₂ NT/MoS₂ nanocomposites. EDS analysis confirms that the atomic ratio between Mo and S in both TiO₂ nanotubes and MoS₂ is close to 1:1.7, consistent with the expected chemical stoichiometry for MoS₂.

The surface topography of TiO₂ NTs with oxidation times of 3 h and 4 h is shown in Figure 4, revealing a distinct separation between each tube opening [20], with an approximate tube diameter of 100 nm. However, upon comparing Figure 4a,b, it becomes evident that the surface of TiO₂ NTs oxidized for 4 h appeared smoother and clearer than that of TiO₂ NTs oxidized for 3 h, indicating superior performance. The fact that the TiO₂ nanotubes were oxidized for 4 h with superior performance indicates a significant enhancement in the effective oxide surface area, as well as the formation of rampant surface defects that may facilitate the adsorption of target molecules, which is beneficial for the gas sensing properties of the TiO₂ NTs.

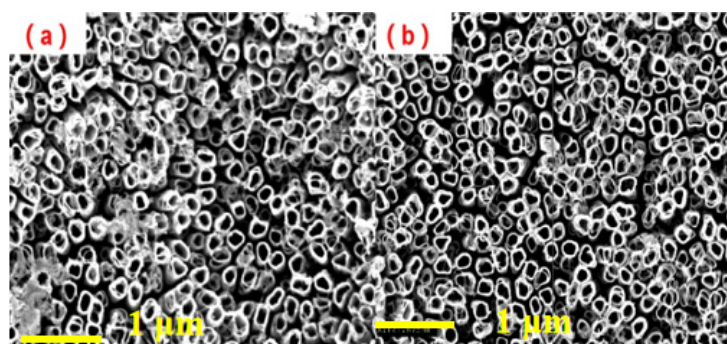


Figure 4. SEM images of TiO₂ NTs with oxidation times of 3 h (a) and 4 h (b).

3.3. Gas-Sensitive Performance of TiO_2 NT/ MoS_2

The response–recovery process curve of pure TiO_2 NTs to four concentrations of NO_2 gas (88 ppm, 146 ppm, 281 ppm, and 369 ppm) at an operating temperature of 260°C is shown in Figure 5. It can be observed that the sensitivity of TiO_2 NTs to gas gradually increased with an increase in NO_2 gas concentration [21], exhibiting sensitivities of 2.8, 3.6, 6, and 9.8, respectively. The response–recovery process curve of TiO_2 NT/ MoS_2 nanocomposites to four concentrations of NO_2 gas (176 ppm, 268 ppm, 367 ppm, and 424 ppm) at an operating temperature of 260°C is presented in Figure 5b. As depicted, the sensitivity of the components to gas progressively improved with an increased NO_2 gas concentration. Moreover, the sensitivity of TiO_2 NT/ MoS_2 composites to NO_2 was higher than that of pure TiO_2 NTs at the same NO_2 concentration. The response time for the TiO_2 NT/ MoS_2 nanocomposites towards 367 ppm NO_2 at 260°C is illustrated in Figure 5c. It can be observed that the components exhibited a rapid response with a 5 s response time and an 80 s recovery time. A potential barrier might form at the MoS_2 and TiO_2 interface due to carrier trapping at the interface, and the potential barrier modulation that occurred during the adsorption and desorption of NO_2 might have positive effects on the sensitivity improvement. The formation of heterojunction near the interface would contribute to the expansion of the depletion layer, which results in an increased change in resistance and enhanced sensitivity [22].

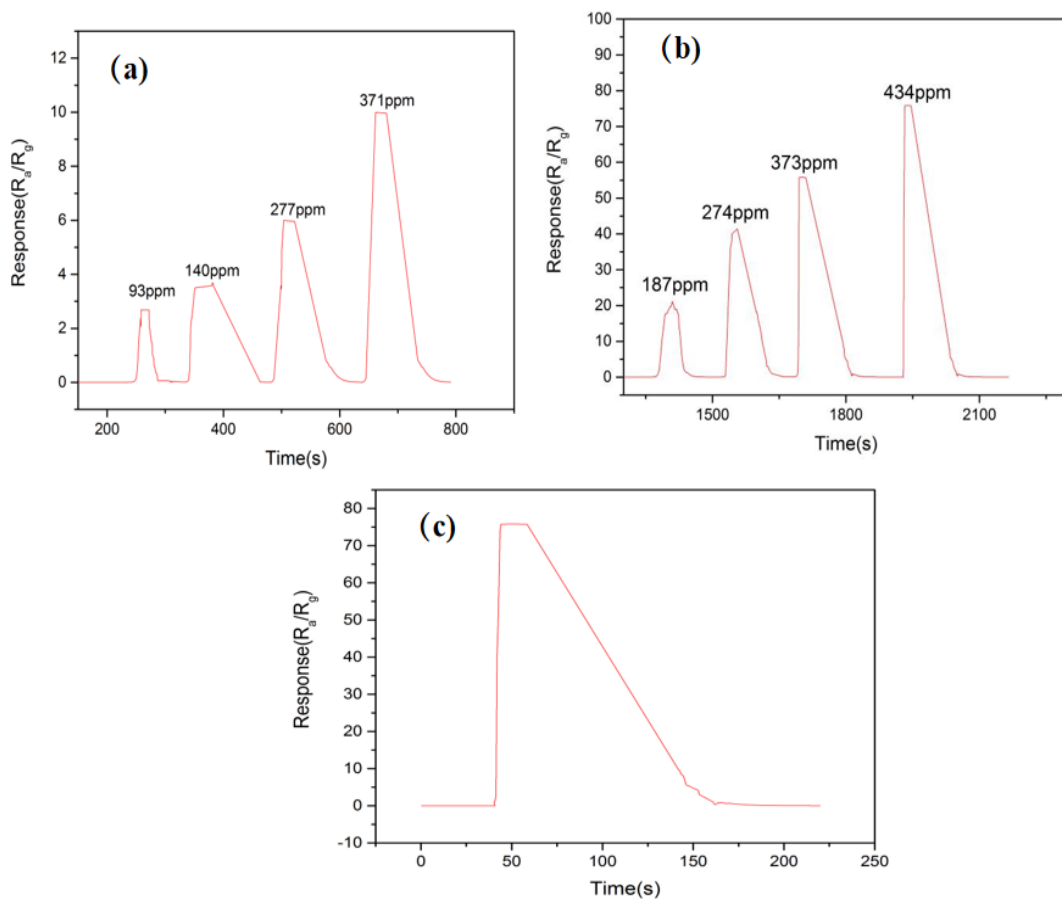


Figure 5. Gas sensitivity tests at 260°C for TiO_2 NTs (a) and TiO_2 NT/ MoS_2 nanocomposites (b) with NO_2 gas concentrations. The response–recovery time curve of TiO_2 NT/ MoS_2 nanocomposites at 260°C with a NO_2 gas concentration of 367 ppm is shown in (c).

Figure 6 shows the responses to several harmful gases at the operating temperature of 260°C . The gas response to 100 ppm NO_2 vapor was found to be 3.3, which is higher than all the other gases under the same concentration. The above results indicate that the

selectivity of the sensor based on TiO₂ NT/MoS₂ nanocomposites is very high and the sensor shows high anti-interference abilities.

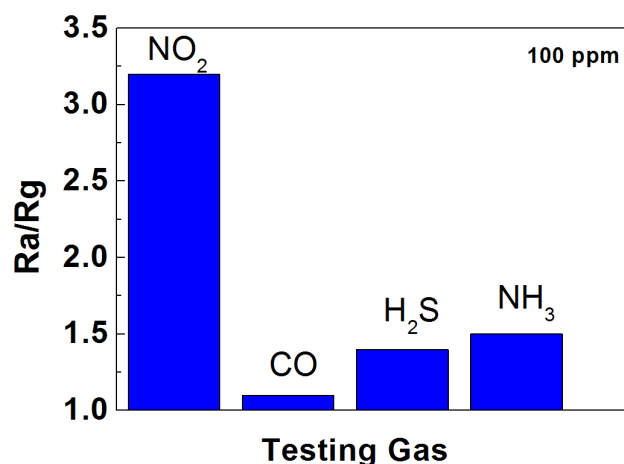


Figure 6. Responses of TiO₂ NT/MoS₂ nanocomposites to 100 ppm of NO₂, CO, H₂S, and NH₃ at 260 °C.

4. Reaction Mechanism for NO₂ Monitoring in the Library

N-type semiconductor materials in the air will interact with oxidizing gases, producing oxidizing particles to absorb oxygen on the surface. The state of the surface adsorbed oxygen is different at any different temperatures. At low temperatures, the gas molecules do not have sufficient thermal energy to react with the surface-adsorbed oxygen species, while at high temperatures, it helps to improve the amount of NO₂ chemisorption, the reaction rate occurring on the TiO₂ surface, and the conductivity behavior of nanocomposites [23]. A larger response arises from the space charge layer due to the oxygen adsorption that penetrates deeper into the TiO₂ nanotubes and MoS₂ can be depleted of carriers through surface interactions, which leads to an increase in the sensing properties. The oxidizing particles will compete for conductive electrons, making the conductivity decrease, and thus forming an electron depletion layer on the surface of the material [24,25]. In this paper, for n-type semiconductor TiO₂ NTs, the TiO₂ NT array was prepared using anodic oxidation method. When the TiO₂ NT array is exposed to NO₂, NO₂ will be directly adsorbed on the surface of TiO₂ NTs and obtain electrons from the conductive band. At the same time, NO₂ molecules will react with O₂ adsorbed on the surface of the material to generate NO₃⁻, increasing the thickness of the depletion layer of TiO₂ NTs and increasing the resistance of the sample. When MoS₂ is doped into the surface of the TiO₂ NT array using hydrothermal method to form the TiO₂ NT/MoS₂ composite, it can be found in the structure and morphology characterization of XRD and SEM that the surface of TiO₂ NTs is attached to the flaky MoS₂, and a large number of flaky MoS₂ layers are gathered together. The TiO₂ NT/MoS₂ composite has a high specific surface area, which can provide more active sites for the adsorption of target gases, indicating that the performance of the TiO₂ adsorption of oxygen ions will be greatly improved. In addition, MoS₂ forms a conductive layer on the surface to improve the electron mobility of TiO₂ [26]. When the material is exposed to the gas NO₂, the adsorption and desorption capacity changes, which leads to the additional modulation of the composite; in other words, the TiO₂ NT/MoS₂ composite exhibits better gas-sensitive response characteristics.

5. Conclusions

NO₂ gas is a significant contributor to the acidification of books and papers, leading to a gradual deterioration in paper quality and mechanical strength over time. In this study, TiO₂ NTs were prepared using the anodic oxidation method, while TiO₂ NT/MoS₂ nanocomposites were synthesized via the hydrothermal method. The MoS₂ nanoparticles

obtained through hydrothermal synthesis exhibited complete coverage on the surface of TiO₂ NTs, resulting in a larger specific surface area compared to pure TiO₂ NTs. After 4 h of oxidation, the diameter of TiO₂ NTs was approximately 100 nm with a smoother and clearer surface morphology. Additionally, the corresponding XRD pattern showed sharper characteristic peaks at this oxidation duration. Gas sensitivity tests conducted at a working temperature of 260 °C demonstrated that the TiO₂ NT/MoS₂ composite exhibited higher sensitivity and selectivity towards different concentrations of NO₂ compared to pure TiO₂ NTs alone. Therefore, the application potential of TiO₂ NT/MoS₂ composite extends to the real-time monitoring of NO₂ gas sensors, as well as preservation techniques for paper books, effectively prolonging their lifespan. Potentially, functionalizing TiO₂ nanotubes with MoS₂, which combines the hierarchical structure of support and the unique properties of MoS₂, opens up new possibilities for flexible and wearable devices for various environmental sensing applications.

Author Contributions: Methodology, J.W. (Jia Wang); Formal analysis, L.K.; Investigation, J.W. (Jieling Wu), F.L. and Y.X.; Writing—original draft, J.W. (Jia Wang). All authors have read and agreed to the published version of the manuscript.

Funding: This work was supported by the Science and Technology Project of Zhanjiang (2022B01044 and 2022A0100).

Institutional Review Board Statement: Not applicable.

Informed Consent Statement: Informed consent was obtained from all subjects involved in the study.

Data Availability Statement: Data are contained within the article.

Conflicts of Interest: The authors declare no conflict of interest.

References

1. Liu, Y. Rational display and preventive protection of books and paper. *Libr. Res. Work.* **2022**, *29*, 29–54.
2. Lu, Y. Air pollution and paper document protection-Analysis of the effects of harmful gases on the durability of paper and protective countermeasures. *Arch. Commun.* **2022**, *29*, 1–9.
3. Cao, G. Research progress on the performance of doped metal oxide semiconductor gas sensor. *Optoelectron. Technol. Appl.* **2020**, *35*, 15–27.
4. Yang, J.; Pan, Y.; Qin, M.; Yan, C.C.; Huang, Q.M. Research progress on metal oxide semiconductor gas sensor. *Chem. Sens.* **2022**, *42*, 10–18.
5. Huang, Y.; Zhou, Q.; Yan, J. Research progress in the application of TiO₂ nanotube array. *Mater. Rev.* **2012**, *26*, 51–54.
6. Dong, J. Design and Application Research of MoS₂/TiO₂ Nanotube Array Composites. Ph.D. Thesis, Soochow University, Suzhou, China, 2019.
7. Feng, H.; Tang, N.; Zhang, S.; Liu, B.; Cai, Q. Fabrication of layered (CdS-Mn/MoS₂/CdTe)-promoted TiO₂ nanotube arrays with superior photocatalytic properties. *J. Colloid Interface Sci.* **2017**, *486*, 58–66. [[CrossRef](#)] [[PubMed](#)]
8. Ye, Z.; Tai, H.; Xie, T.; Yuan, Z.; Liu, C.; Jiang, Y. Room temperature formaldehyde sensor with enhanced performance based on reduced graphene oxide/titanium dioxide. *Sens. Actuators B Chem.* **2016**, *223*, 149–156. [[CrossRef](#)]
9. Sennik, E.; Alev, O.; Öztürk, Z.Z. The effect of Pd on the H₂ and VOC sensing properties of TiO₂ nanorods. *Sens. Actuators B Chem.* **2016**, *229*, 692–700. [[CrossRef](#)]
10. Shao, Z.; Liu, W.; Zhang, Y.; Yang, X.; Zhong, M. Insights on interfacial charge transfer across MoS₂/TiO₂-NTAs nanoheterostructures for enhanced photodegradation and biosensing & gas-sensing performance. *J. Mol. Struct.* **2021**, *1244*, 131240.
11. Zhang, D.; Jiang, C.; Zhou, X. Fabrication of Pd-decorated TiO₂/MoS₂ ternary nanocomposite for enhanced benzene gas sensing performance at room temperature. *Talanta* **2018**, *182*, 324–332. [[CrossRef](#)]
12. Singh, S.; Raj, S.; Sharma, S. Ethanol sensing using MoS₂/TiO₂ composite prepared via hydrothermal method. *Mater. Today Proc.* **2021**, *46*, 6083–6086. [[CrossRef](#)]
13. Zhao, P.X.; Tang, Y.; Mao, J.; Chen, Y.X.; Song, H.; Wang, J.W.; Song, Y.; Liang, Y.Q.; Zhang, X.M. One-Dimensional MoS₂-Decorated TiO₂ nanotube gas sensors for efficient alcohol sensing. *J. Alloys Compd.* **2016**, *674*, 252–258. [[CrossRef](#)]
14. Tian, X.; Cui, X.; Xiao, Y.; Chen, T.; Xiao, X.; Wang, Y. Pt/MoS₂/Polyaniline Nanocomposite as a Highly Effective Room Temperature Flexible Gas Sensor for Ammonia Detection. *ACS Appl. Mater. Interfaces* **2023**, *15*, 5091110. [[CrossRef](#)] [[PubMed](#)]
15. Shou, Y.; Zhao, J.; Qiao, J. Preparation of SnO₂-Based Composite Gas-Sensitive Material and Its Effect on the Membrane Treatment Process of Volatile Organic Compounds. *J. Nanomater.* **2022**, *2022*, 5091110. [[CrossRef](#)]
16. Zhao, Y.; Chang, C.; Chen, L.; Ma, J.; Xiong, C. Study on the controllable preparation of TiO₂ nanotube arrays by anodic oxidation method. *Chem. Eng.* **2018**, *32*, 18–21.

17. Li, H.; Chen, Y.; Zheng, X.; Zu, G.; Chang, Y.; Wu, Y. Preparation and application of TiO₂ nanotubes. *Met. Funct. Mater.* **2022**, *29*, 1–9.
18. Chen, Y.; He, D.; Wang, Y.; Yang, B. Preparation of TiO₂-graphene composite photocatalyst by hydrothermal method and its photocatalytic performance. *Acta Lumines* **2019**, *40*, 177–182.
19. Huang, D.; Mo, Z.; Quan, S.; Yang, T.; Liu, Z.; Liu, M. Preparation and photocatalytic reduction performance of graphene/nano-TiO₂ composites. *J. Compos.* **2016**, *33*, 155–162.
20. Tan, Z.; Wang, H.; Yang, H.; Zhang, X. Morphology of TiO₂ nanotube arrays prepared by anodic oxidation method. *J. Mater. Sci. Eng.* **2013**, *31*, 390–394.
21. Sushmitha, V. Ti@MoS₂ incorporated Polypropylene/Nylon fabric-based porous, breathable triboelectric nanogenerator as respiration sensor and ammonia gas sensor applications. *Sens. Actuators B Chem.* **2023**, *380*, 133346.
22. Singh, S.; Sharma, S. Temperature dependent selective detection of ethanol and methanol using MoS₂/TiO₂ composite. *Sens. Actuators B Chem.* **2022**, *350*, 130798. [[CrossRef](#)]
23. Shooshtari, M.; Salehi, A.; Vollebregt, S. Effect of temperature and humidity on the sensing performance of TiO₂ nanowire-based ethanol vapor sensors. *Nanotechnology* **2021**, *32*, 325501. [[CrossRef](#)] [[PubMed](#)]
24. Tian, K. Preparation of Metal Oxide Semiconductor Heterojunction and Its Gas Sensing and Photoelectrochemical Properties and Mechanism. Master's Thesis, Beijing University of Chemical Technology, Beijing, China, 2023.
25. Bu, X.; Bao, S.; Chu, X.; Liang, S.; Wang, C.; Bai, Y. Preparation and gas sensing properties of MoS₂/Cd₂SnO₄ composites. *Acta Inorganica Sin.* **2022**, *38*, 2173–2180.
26. Zou, C.; Wang, J.; Xie, W. Synthesis and enhanced NO₂ gas sensing properties of ZnO nanorods/TiO₂ nanoparticles heterojunction composites. *J. Colloid Interface Sci.* **2016**, *478*, 22–28. [[CrossRef](#)]

Disclaimer/Publisher's Note: The statements, opinions and data contained in all publications are solely those of the individual author(s) and contributor(s) and not of MDPI and/or the editor(s). MDPI and/or the editor(s) disclaim responsibility for any injury to people or property resulting from any ideas, methods, instructions or products referred to in the content.